Redox Biology 80 (2025) 103510

Contents lists available at ScienceDirect

Redox Biology

journal homepage: www.elsevier.com/locate/redox

Melatonin protects aged oocytes from depalmitoylation-mediated quality reduction by promoting PPT1 degradation and antioxidation

Rujun Ma [a,b,c,1], Mengqi Xue [a,b,1], Feiyan Ge [a,1], Kadiliya Jueraitetibaike [a,1], Shanmeizi Zhao [a], Zhang Qian [a], Zhaowanyue He [a], Hong Zhang [a], Ting Tang [a], Chun Cao [c], Chuwei Li [a], Lu Zheng [a], Tongmin Xue [d], Jie Dong [a], Jun Jing [a,b], Jian Zhong [e], Jinzhao Ma [a], Yang Yang [f], Yadong Huang [g,h,**], Xie Ge [a,c,***], Bing Yao [a,b,c,****], Li Chen [a,b,c,*]

[a] Department of Reproductive Medicine, Jinling Hospital, Affiliated Hospital of Medical School, Nanjing University, Nanjing, Jiangsu, 210002, China
[b] State Key Laboratory of Reproductive Medicine and Offspring Health, Nanjing Medical University, Nanjing, Jiangsu, 211166, China
[c] Department of Reproductive Medicine, Affiliated Jinling Hospital, The First School of Clinical Medicine, Southern Medical University, Nanjing, 210002, China
[d] Reproductive Medical Center, Clinical Medical College (Northern Jiangsu People's Hospital), Yangzhou University, Yangzhou, Jiangsu, 225001, China
[e] Department of Gynecology, Women's Hospital of Nanjing Medical University, Nanjing, Jiangsu, 210004, China
[f] Clinical Laboratory, Nanjing Jinling Hospital, Affiliated Hospital of Medical School, Nanjing University, Nanjing, Jiangsu, 210002, China
[g] Department of Cell Biology, Jinan University, Guangzhou, 510632, China
[h] Guangdong Province Key Laboratory of Bioengineering Medicine, Guangzhou, 510632, China

ARTICLE INFO

Keywords:
Oocyte aging
Melatonin
Antioxidation
Palmitoyl-protein thioesterase 1
Palmitoylation
Tubulin

ABSTRACT

Oocyte aging is closely related to a decline in female fertility, accompanied by increased reactive oxygen species levels and changes in protein posttranslational modifications. However, the role of protein palmitoylation in oocyte aging has not been investigated. In the present study, a new association between redox and palmitoylation in aging oocytes was found. We found that the protein level of palmitoyl-protein thioesterase 1 (PPT1), a depalmitoylation enzyme, was increased in maternally aged mice oocytes and follicular fluid of aged (age >35 years) patients with decreased ovarian reserve (DOR). Elevated PPT1 led to decreased S-palmitoylation levels in oocytes, which impaired oocyte maturation and spindle formation. Tubulin was identified as a critical palmitoylated protein regulated by PPT1, whose palmitoylation was also decreased by advanced age, accompanied by abnormalities in membrane localization and microtubule polymerization. Melatonin was found to down-regulate excessive PPT1 and rescue PPT1-induced damage in mouse oocytes, not only by regulating oxidative stress, but also by binding with PPT1 to regulate its lysosomal degradation. In summary, our data demonstrate that PPT1 participates in oocyte aging by regulating tubulin palmitoylation, providing evidence that oxidative stress regulates protein palmitoylation and revealing a novel mechanism of oocyte aging.

1. Introduction

Reduced oocyte quality is an important reason for the decline in reproductive ability in aging women. A variety of detrimental physiological changes in oocytes, such as increased reactive oxygen species (ROS) levels, DNA damage, chromosome aneuploidy, mitochondrial

* Corresponding authors. Department of Reproductive Medicine, Jinling Hospital, Affiliated Hospital of Medical School, Nanjing University, Nanjing, Jiangsu, China.
** Corresponding author. Department of Cell Biology, Jinan University, Guangzhou, China.
*** Corresponding authors. Department of Reproductive Medicine, Jinling Hospital, Affiliated Hospital of Medical School, Nanjing University, Nanjing, Jiangsu, China.
**** Corresponding author. Department of Reproductive Medicine, Jinling Hospital, Affiliated Hospital of Medical School, Nanjing University, Nanjing, Jiangsu, China.
E-mail addresses: tydhuang@jnu.edu.cn (Y. Huang), gexie85@163.com (X. Ge), yaobing@nju.edu.cn (B. Yao), chenli1978@nju.edu.cn (L. Chen).
[1] These authors contributed equally: Rujun Ma, Mengqi Xue, Feiyan Ge, Kadiliya Jueraitetibaike.

https://doi.org/10.1016/j.redox.2025.103510
Received 14 November 2024; Received in revised form 18 January 2025; Accepted 20 January 2025
Available online 21 January 2025

dysfunction, and abnormal lipid metabolism can be caused by aging [1–6]. Additionally, oocyte aging is also accompanied by changes in protein posttranslational modifications, such as acetylation [7], methylation [8], and ubiquitination [9]. Interestingly, S-palmitoylation consists of the attachment of a palmitic acid residue to a cysteine residue by a potentially reversible thioester linkage, which is related to lipid metabolism in the body [6,10] and can be regulated by ROS [11]. Thus, abnormal lipid metabolism and ROS level in oocyte aging might also induce alteration of protein palmitoylation. In the aging brains of both humans and nonhuman primates, a reduction in DHHC5-mediated Beclin 1 S-palmitoylation is implicated in the decline of autophagy [12]. Furthermore, in aging males with LOH, a notable decrease in global protein palmitoylation in peripheral blood is observed, regulated by the miR-125a-5p/LYPLA1 signaling pathway [13]. These researches collectively suggest that age-related reductions in palmitoylation may play a crucial role in the pathogenesis of the disease. Few studies have reported the function of palmitoylation in oocytes. The palmitoylation of Ha-Ras has been reported to facilitate meiotic maturation in Xenopus oocytes [14]. When ZDHHC3-mediated palmitoylation of Gs alpha is reduced, oocytes are not arrested at G2 in Xenopus [15]. The role of alterations in protein palmitoylation in oocyte aging remains to be investigated.

Protein S-palmitoylation is catalyzed by acyl transferases (zDHHC domain-containing proteins), and depalmitoylation is mediated by acyl protein thioesterases (for example, APT1, APT2, ABHD family members and palmitoyl-protein thioesterase 1 (PPT1)). PPT1, the first depalmitoylation enzyme identified, mediates the depalmitoylation of various proteins, such as H-Ras and CSPα [16,17], and is involved in the regulation of transmembrane receptors, signaling proteins, and many other molecules [18]. Mutations in PPT1 lead to autosomal recessive brain disorders and infantile neuronal ceroid lipofuscinosis [19,20]. MacDonald ME et al. demonstrated that abnormal elevation of PPT1 levels can cause neuronal cell death [21]. In recent years, decreased fertility caused by the upregulation of PPT1 has also been reported. It was found that increased PPT1 levels in rats fed a high-fat diet (HFD) result in reduced male fertility [22]. Our previous study revealed that PPT1 participates in the pathogenesis of hyperandrogenism by regulating HSP90α depalmitoylation [23]. The precise regulation of PPT1 expression is very important for cells. PPT1 can be upregulated by mitochondrial oxidative stress [24], which is known to occur during oocyte aging and has a significant negative effect on oocyte quality [25,26]. However, the role of PPT1 in oocyte meiosis and aging has not been reported.

Melatonin (5-methoxy-N-acetyltryptamine), a pleiotropic hormone secreted by the pineal gland, is known to have anti-aging properties related to its antioxidant and anti-inflammatory actions [27,28]. High concentrations of melatonin exert positive effects on oocyte quality. Clinical studies have shown that prophylactic oral melatonin treatment can increase the number of mature oocytes and the percentage of high-quality embryos following subsequent IVF or ICSI [29]. Maternal aging induces the loss of melatonin in both the blood serum and follicular fluid, which leads to meiotic failure in oocytes [30]. Melatonin supplementation has been shown to protect oocytes from advanced maternal age-associated meiotic defects in both *in vivo* and *in vitro* models [30–32]. However, the mechanism underlying these effects remains to be further explored. Whether melatonin regulates oocyte aging by targeting PPT1 and protein palmitoylation is the focus of this study.

In the present study, we discovered that ROS-induced overexpression of PPT1 in aged oocytes resulted in tubulin depalmitoylation and spindle defects. Moreover, melatonin increased the level of tubulin palmitoylation by inhibiting PPT1 and subsequently promoted meiotic maturation and improved oocyte quality in aged mice.

2. Results

2.1. Elevated PPT1 in maternal aging ovary is associated with poor oocyte quality

Since ovarian aging occurs earlier than other organs [33], we performed western blot analysis of the ovary, brain, heart, liver, and muscle from control (6–8-week-old) and aged (8–10-month-old) mice, respectively. Interestingly, we found that PPT1 levels increased in ovaries, but not other tissues, from aged mice, compared to those from young controls (Fig. 1A and Fig. S1A and B). As shown in Fig. 1B, we also increased PPT1 expression levels in oocytes isolated from aged mouse ovary. To further determine the cellular events in which PPT1 is involved in meiotic maturation, we examined its localization at different stages of mouse oocyte development using immunofluorescence. As shown in Fig. 1C and Fig. S1C, at the GV stage, PPT1 resided in the membrane and cytoplasm of oocytes and exhibited vesicular localization in the nucleus. Remarkably, as the oocytes entered metaphase, PPT1 became concentrated on the spindle region. Clear overlap of fluorescence signals was observed in oocytes in metaphase labeled with both anti-PPT1 and anti-α-tubulin antibodies, indicating that PPT1 was enriched at the meiotic spindle (Fig. 1D). While the expression of PPT1 did not change significantly during oocyte mitosis (Fig. S1D), the alterations in localization may be more relevant to its function.

To explore the function of PPT1 in oocyte aging, we injected exogenous PPT1 mRNA into young mouse oocytes arrested in the GV stage with milrinone and incubated them for 20 h to synthesize new PPT1 protein (called the oePPT1 group). The oocytes were then washed and allowed to mature in normal medium or medium containing 1 μM melatonin. After PPT1 mRNA injection for 20 h, increased PPT1 was confirmed by using quantitative real-time PCR (RT-PCR) analysis and western blotting (Fig. 1E and F). Then, we observed the Pb1 extrusion rate in the control and oePPT1 groups. Only 33.37 % of oePPT1 oocytes ($n = 173$) extruded Pb1 at 14 h, and this percentage was significantly lower than that observed for control oocytes (80.08 %, $n = 135$; Fig. 1G). This result suggested that PPT1 overexpression significantly inhibited oocyte maturation.

Furthermore, we measured the protein level of PPT1 in human ovaries, which were divided into young and aged groups according to donor age. A significant increase in PPT1 levels with age was detected (Fig. 1H). The ages of the donors are shown in Supplementary Fig. 1E. Then, the protein level of PPT1 in follicular fluid by ELISA. The PPT1 protein expression in aged-DOR group were significantly higher than those in young group and aged-control group (Fig. 1I). These results implied that PPT1 expression changes are age-related and may be associated with alterations in female fertility.

2.2. Melatonin prevents PPT1 overexpression in aged oocytes

Oxidative stress has been reported to promote PPT1 expression [24]. Moreover, as described in our previous article, 50 μM hydrogen peroxide (H_2O_2) was used for 14 h during *in vitro* maturation (IVM) to simulate oxidative stress during oocyte aging [34]. Western blotting showed that H_2O_2 treatment led to a significant increase in PPT1 protein expression in oocytes (Fig. 2A). Melatonin, a classic antioxidant, attenuated H_2O_2-induced oxidative stress and decreased PPT1 levels (Fig. 2A and Fig. S1F). This finding suggested that melatonin can regulate PPT1 expression under oxidative stress condition.

To clarify the regulatory effect of melatonin on PPT1 levels in aged oocytes, female mice were orally administered melatonin (the aged + mel/i.g. group) as previously described in the published literature [31] (Fig. 2B). We first examined melatonin and sex hormone concentrations in the blood serum of control, aged and aged + mel/i.g. mice by ELISA. The serum levels of melatonin and anti-Mullerian hormone (AMH) were lower in aged mice than in control mice (Fig. 2C and Fig. S2A). Melatonin supplementation significantly increased the serum melatonin

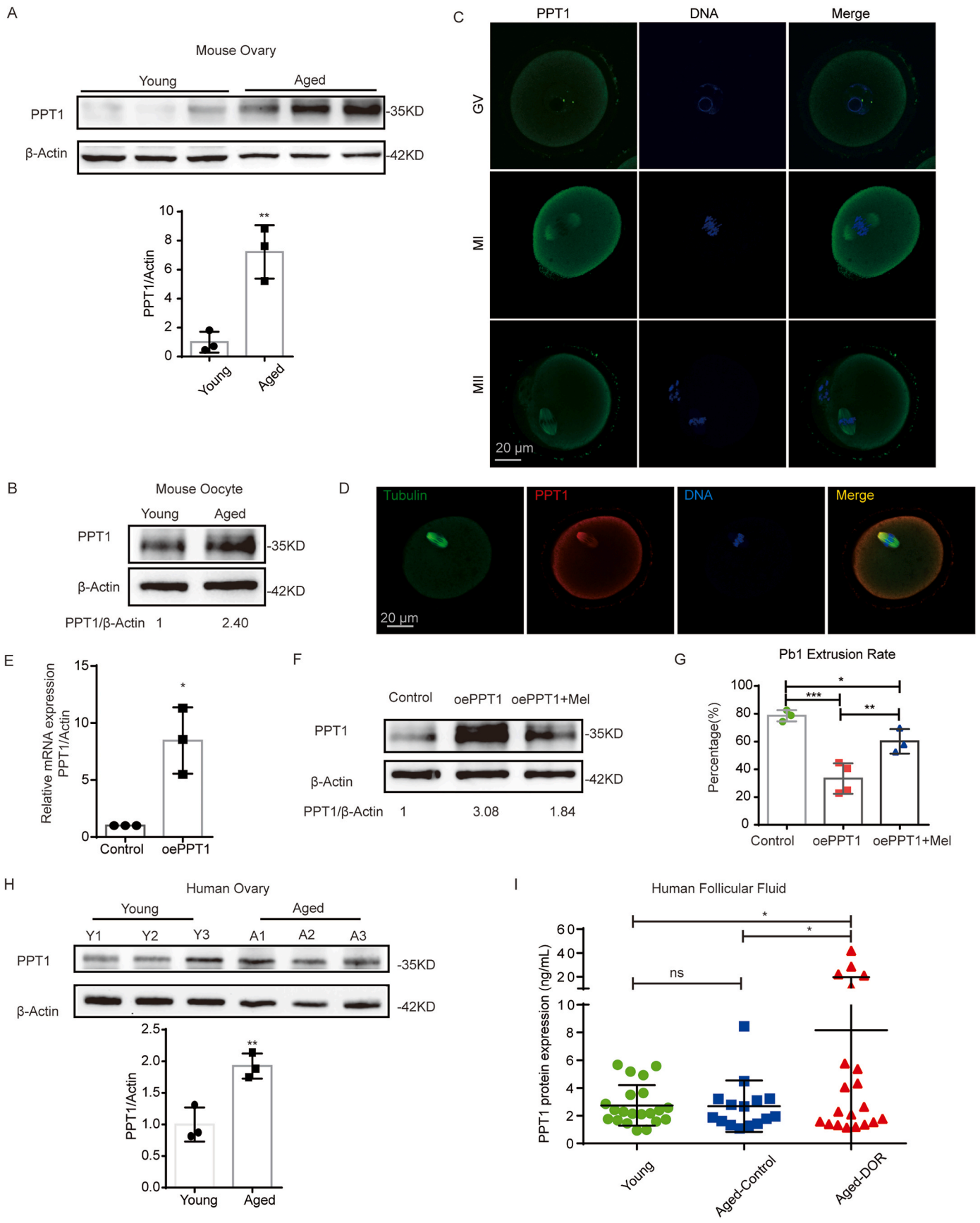

(caption on next page)

Fig. 1. The expression of PPT1 in the ovary is correlated with age. (A) Western blot analysis showing PPT1 expression in ovaries from control and aged mice. (B) Western blot analysis showing PPT1 expression in mouse oocytes from control and aged mice. (C) Immunofluorescence staining was used to assess the subcellular localization of PPT1. Green, PPT1; blue, chromatin. (D) Immunofluorescence colocalization analysis of tubulin and PPT1 in mouse oocytes during the MI phase. Red, PPT1; green, tubulin; blue, chromatin. (E) The relative mRNA level of PPT1 in control and PPT1-mRNA-injected (called the oePPT1 group) oocytes was determined by quantitative RT-PCR. The mRNA level in control oocytes was set to 1. (F) Western blot analysis showing PPT1 expression in oocytes from mice in the control, oePPT1 and oePPT1+mel groups. (G) Pb1 extrusion rate in the control (n = 135), oePPT1 (n = 173) and oePPT1+mel (n = 218) groups. (H) Western blot analysis showing PPT1 expression in young (n = 3) and aged (n = 3) donor ovaries. (I) The results of PPT1 ELISA showed that the PPT1 protein expression in follicular fluid of young (n = 21), aged-control (n = 13) and aged-DOR (n = 25) donors. β-Actin served as a loading control for Western blotting. The data are presented as the means ± SDs from three independent experiments. $^{*}p < 0.05$, $^{**}p < 0.01$, and $^{***}p < 0.001$.

content in the aged group (Fig. 2C), while there was no significant difference in the levels of sex hormones, including AMH, E2, P, FSH and LH (Figs. S2A–F). These results suggested that melatonin has little effect on the secretion of sex hormones. Analysis of the follicle count by HE staining revealed that exogenous melatonin supplementation significantly increased the number of secondary follicles in aged mice (Figs. S2G–H), suggesting that melatonin can rescue ovarian function in aged mice.

Then, we assessed the expression of PPT1 in oocytes from control, aged and aged + mel/i.g. mice by western blotting. PPT1 expression was significantly higher in both the oocytes and ovaries of aged mice than in those of control mice, and these changes were reversed by melatonin administration (Fig. 2D and Fig. S2I). We also applied melatonin to aged oocytes during IVM and measured the expression of PPT1 after 14 h of IVM. Similarly, the increase of PPT1 level in aged oocytes was inhibited by melatonin treatment during IVM (Fig. 2E). These results suggest that high expression of PPT1 may play a role in oocyte aging and can be regulated by melatonin.

2.3. Melatonin can bind to PPT1 and promote its lysosomal degradation

We found that melatonin ameliorated the abnormally high PPT1 levels (Fig. 1F) and increased the rate of polar body extrusion in oePPT1 oocytes (59.91 %, n = 163; Fig. 1G). This result suggested that melatonin can regulate PPT1 expression in a manner other than antioxidation. To evaluate the affinity of melatonin for PPT1, we performed molecular docking analysis by Antodock Vina v.1.2.2. For PPT1, melatonin had low binding energy of −6.548 kcal/mol, indicating a stable binding (Fig. 2F). Surface Plasmon Resonance (SPR) assay determined that PPT1 can bind to melatonin with an affinity constant of 0.007511 M (Fig. 2G). Above results confirmed that melatonin could directly bind to PPT1 protein.

PPT1 is a lysosomal enzyme. Since we discovered that melatonin reverses abnormal lysosomal accumulation in aged oocytes (Fig. 2H and I), we tested the involvement of lysosomal degradation in PPT1 regulation. We treated HEK293T cells with lysosome inhibitor chloroquine (CQ) or the protein synthesis inhibitor cycloheximide (CHX) after PPT1 overexpression and melatonin modulation. The PPT1 level decreased to a low basal level after CHX treatment, but still increased when CHX treatment was coupled with oePPT1 or decreased when CHX treatment was coupled with additional melatonin, suggesting that protein degradation is a main regulatory mechanism of melatonin for PPT1 (Fig. 2J). We found that CQ upregulated PPT1 to similar levels in oePPT1 and oePPT1 plus melatonin, pointing to a lysosome-dependent mechanism (Fig. 2J).

2.4. The global S-palmitoylation levels play an important part in mouse oocyte meiosis

Because PPT1 is a depalmitoylation enzyme, we analyzed the global S-palmitoylation level in oocytes by an acyl-biotin exchange (ABE) assay (Fig. 3A). First, we observed decreased palmitoylation in aged oocytes (Fig. 3B). The global S-palmitoylation level in oocytes collected from aged + mel/i.g. mice was significantly greater than that in oocytes collected from aged mice (Fig. 3B). Similar results were observed after melatonin treatment during IVM (Fig. 3C). Melatonin treatment also reversed the H_2O_2-induced reduction in the palmitoylation level in oocytes (Fig. 3D). Next, palmitoylation levels were measured in oocytes after PPT1 overexpression. When PPT1 was overexpressed, the palmitoylation levels decreased significantly, and this change was reversed by melatonin treatment (Fig. 3E). These results indicated that PPT1 is critical for maintaining palmitoylation levels in oocytes.

In addition, we measured the global S-palmitoylation level in mouse ovaries and HEK293T cells. The palmitoylation levels in ovaries from the control, aged and aged + mel/i.g. groups showed a similar trend to that observed for oocytes from these same groups of mice (Fig. S3A). Similarly, the overexpression of PPT1 in HEK293T cells reduced the total palmitoylation level (Figs. S3B and C). These results suggest that PPT1 has a similar regulatory effect on global S-palmitoylation in oocytes, ovaries and HEK293T cells.

To further determine whether the deficiency in palmitoylation caused by high PPT1 levels plays an important role in oocyte meiotic defects, the palmitoylation inhibitor 2-bromopalmitate (2BP) was used to inhibit palmitoylation in oocytes. Treatment with 25 μM 2BP (the dose was selected according to the data shown in Fig. S3D) significantly reduced the palmitoylation level (Fig. 3F) and maturation rate of mouse oocytes (43.02 % vs. 81.64 % control; Fig. 3G and H) but had no effect on the GVBD rate (Fig. 3H). Interestingly, melatonin was also found to counteract the decline in oocyte maturation rate induced by 2BP treatment (67.12 % vs. 43.02 % 2BP treatment; Fig. S3E). Therefore, precisely modulated palmitoylation level is necessary for the maintenance of oocyte maturation rate.

2.5. Proper palmitoylation is essential for spindle organization in oocytes

Since the upregulation of PPT1 or inhibition of palmitoylation lead to impairment of oocyte maturation (Figs. 1G and 3H), we assessed the spindle morphology and chromosome alignment by immunofluorescence. Oocytes were immunolabeled with an anti-tubulin antibody to visualize the spindle and co-stained with propidium iodide to visualize chromosomes. Confocal microscopy revealed that most control oocytes at metaphase presented with a typical barrel-shaped spindle and well-aligned chromosomes on the metaphase plate. Compared to control group, a markedly elevated rate of abnormal spindle morphology and chromosome alignment was readily observed in 2BP-treated oocytes (31.29 % vs. 8.17 % control; Fig. 4A and B). The oocytes in the oePPT1 group also displayed a high frequency of spindle defects and chromosome disorganization (20.8 % vs. 8.69 % control; Fig. 4D and E), mainly including diverse malformed spindles and the displacement of one or several chromosomes from the equator. Melatonin supplementation rescued the damage caused by 2BP treatment (19.52 % vs. 31.29 % 2BP treatment; Figs. S3F and G) and PPT1 overexpression (13.34 % vs. 20.8 %; Fig. 4D and E).

Moreover, oocytes in the 2-BP treated or oePPT1 group had thicker spindles. The merged images taken by Z-stack were used to measure the width of the spindle. The widest distance in the middle of the spindle was measured as the width. On average, the metaphase spindle widths of 2-BP treated and oePPT1 oocytes were 30 % wider than those of control oocytes (Fig. 4C and F), while there was no difference between the melatonin group and the control group.

We observed that the spindle defects and chromosome misalignment following PPT1 overexpression (Fig. 4Db, c) were similar to those of

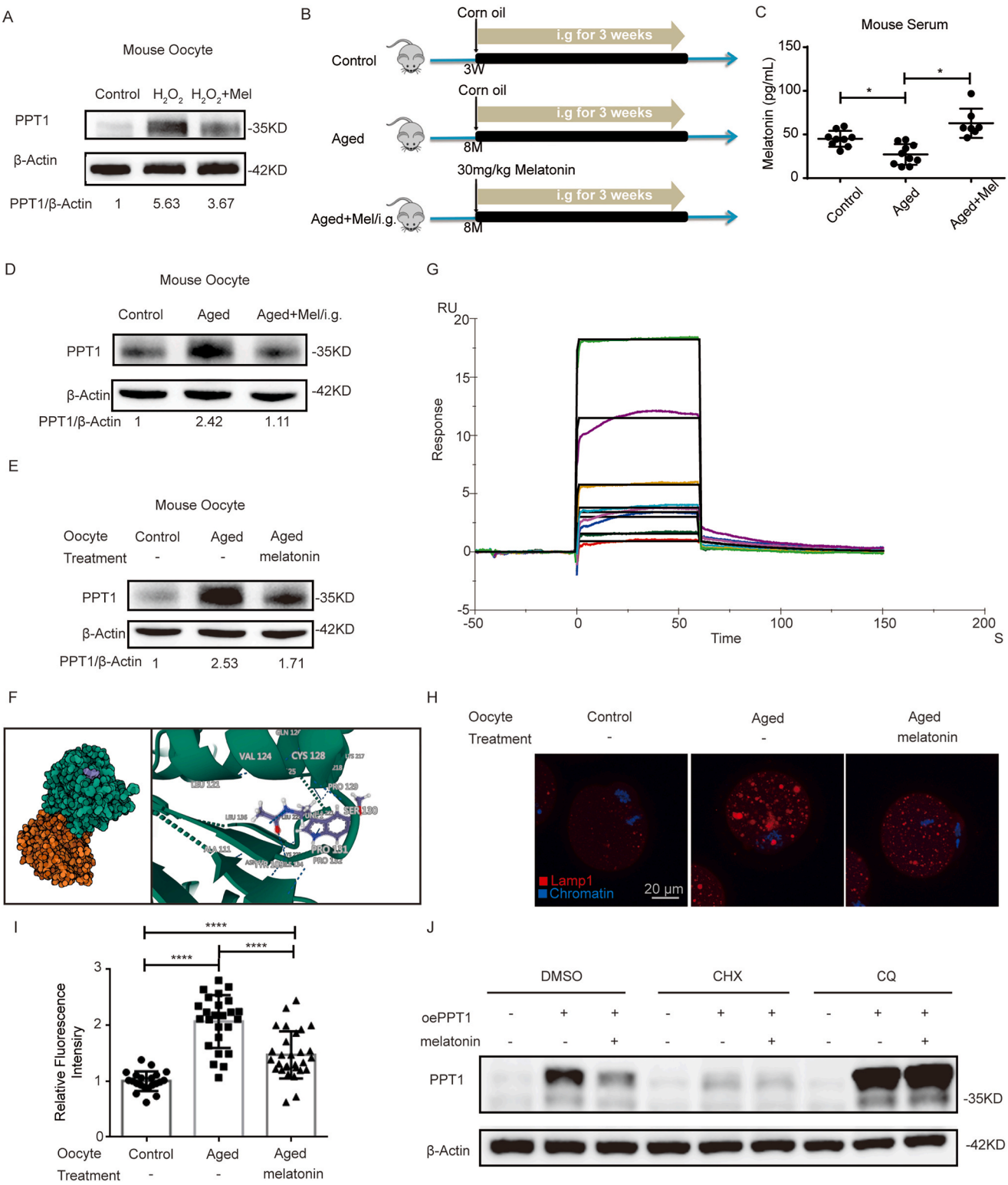

Fig. 2. Effects of melatonin on PPT1 expression in oocytes and ovaries during maternal aging. (A) Western blot analysis showing PPT1 expression in oocytes in the control, H_2O_2 and H_2O_2 + mel groups. (B) Timeline of melatonin administration to mice. (C) The level of melatonin in the blood serum of young mice (n = 9), aged mice (n = 10) and melatonin-treated mice (n = 7). (D) Western blot analysis showing PPT1 expression in oocytes from control, aged and aged + mel/i.g. mice. (E) Western blot analysis showing PPT1 expression in oocytes from control, aged and melatonin-treated mice. (F) Binding mode of melatonin to PPT1 by molecular docking. (G) PPT1, mouse (HEK293, His) can bind melatonin with an affinity constant of 0.007511 M as determined in SPR assay. (H) Oocytes in the control, aged and aged + mel groups were collected and stained to visualize lysosome (red) and chromosomes (blue). Scale bar, 20 μm. (I) The relative fluorescence intensity in the control (n = 21), aged (n = 25) and aged + mel (n = 29) groups based on the area of Lamp1 signals.(J) The expression level of PPT1 in HEK293T cells treated with PPT1-HA, oePPT1 plus melatonin, or additionally treated with CQ or CHX. β-Actin served as a loading control for Western blotting. The data are presented as the means ± SDs from three independent experiments. *$p < 0.05$, ****$p < 0.0001$.

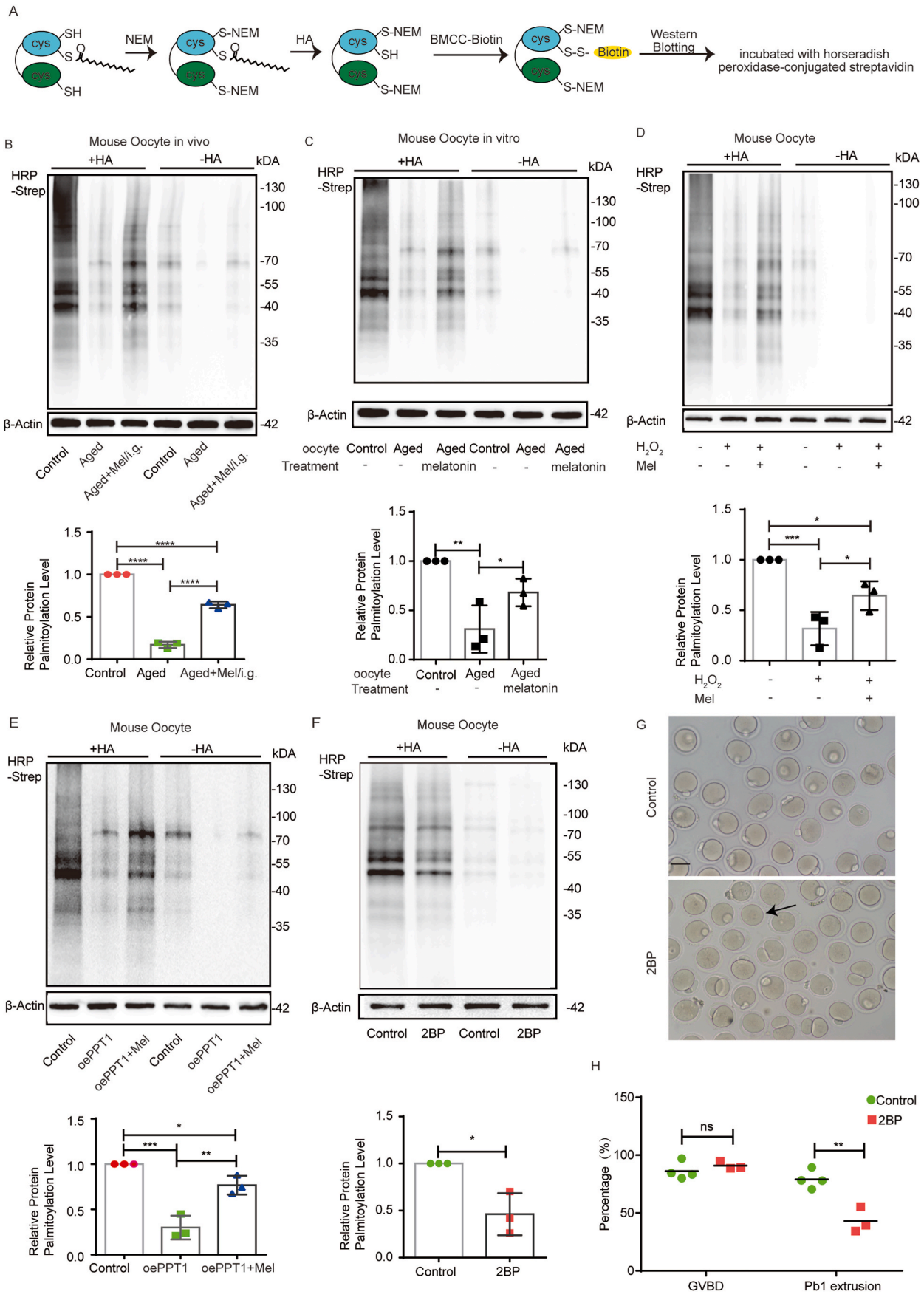

(caption on next page)

Fig. 3. Global S-palmitoylation levels in oocytes were regulated by PPT1 and melatonin. (A) Schematic of ABE for detecting global protein S-palmitoylation. (B) Analysis of the palmitoylation levels of proteins extracted from oocytes from control, aged and aged + mel/i.g. mice. (C) Analysis of the palmitoylation levels of proteins extracted from control and aged oocytes with or without melatonin treatment. (D) Analysis of the palmitoylation levels of proteins extracted from control, H_2O_2 and H_2O_2 + mel oocytes. (E) Analysis of the palmitoylation levels of proteins extracted from oocytes in the control, oePPT1 and oePPT1 + mel groups. (F) Analysis of the palmitoylation levels of proteins extracted from control and 2BP-treated (called the 2BP) oocytes. (G) Representative phase contrast images of MII oocytes from the control and 2BP groups. Scale bar, 50 μm. (H) Pb1 extrusion rates of control (n = 240) and 2BP-treated oocytes (n = 301). Actin served as a loading control for ABE assay. The data are presented as the means ± SDs from three independent experiments. *$p < 0.05$, **$p < 0.01$, ***$p < 0.001$, and ****$p < 0.0001$.

aged oocytes (Fig. 5Db, c). Subsequently, we performed knockdown experiments to test whether decreased PPT1 expression in aged oocytes could rescue meiotic defects. We microinjected PPT1-siRNA into fully grown oocytes (called siPPT1), and quantitative RT-PCR and western blot analysis revealed a significant reduction in PPT1 mRNA and protein levels (Fig. 5A and B). The knockdown of PPT1 in aged mouse oocytes can raised the total palmitoylation level (Fig. 5C). Immunofluorescence showed that the proportion of spindle defects in oocytes from the siPPT1 group decreased significantly compared with that in oocytes from the aged group (16.71 % vs. 25.20 %, Fig. 5D and E). The width of the spindle in oocytes from the siPPT1 group showed recovery trends compared with those in oocytes from the aged group (Fig. 5F), indicating that PPT1 knockdown partly reversed the meiotic defects in aged oocytes.

2.6. Melatonin ameliorates tubulin dysfunction by regulating tubulin palmitoylation

As we found that the change in PPT1 expression in oocytes is consistent with that in ovaries during aging, we used ovaries in place of oocytes for some experiments that require large amounts of proteins, such as mass spectrometry (MS) and ABE assays using HPDP-biotin. First, we pulled down proteins from mouse ovary lysates with an anti-PPT1 antibody and used the proteins for MS (Fig. 5G). Based on the MS results, tubulin alpha 1A, tubulin alpha 1B and tubulin beta 5 directly bound to PPT1 (Fig. 5H).

Based on the MS results, Cys12 and Cys354 of tubulin beta 5 were identified as possible cysteine sites for PPT1 binding. Representative spectra of tubulin alpha 1B and tubulin beta 5 are shown in Fig. 5I–J. Although tubulin alpha 1A and tubulin alpha 1B was analyzed by MS, there was no cysteine site in the identified peptides. Then, we predicted the palmitoylation sites in tubulin beta 5 using GPS-PALM software (https://www.biocuckoo.org/). The identified potential palmitoylation sites are shown in Fig. S4A and include Cys12 and Cys354 of tubulin beta 5. Thus, Cys12 and Cys354 of tubulin beta 5 are potential palmitoylation sites targeted by PPT1. Sequence alignment of tubulin beta 5 around Cys12 and Cys354 among different species showed that these palmitoylation sites have a high degree of homology across species (Fig. S4B).

Then, the tubulin palmitoylation level was analyzed, and an ABE assay using HPDP-biotin was performed (Fig. 6A). Tubulin palmitoylation was decreased in the ovaries of aged mice compared with those of control mice, and this change was reversed in the ovaries of aged + mel/i.g. mice (Fig. 6B). The actin palmitoylation level did not differ among ovaries from the control, aged and aged + mel/i.g. groups (Fig. 6C). These results indicate that a decreased tubulin palmitoylation level may be involved in aging.

HEK293T cells were used for further confirmation. As expected, 2BP induced tubulin depalmitoylation (Fig. 6D). Moreover, 50 mmol/L D-gal was used to induce cell senescence [35], which also caused a decrease in the palmitoylation level of tubulin (Fig. S4C), revealing that HEK293T cells can be used as a practical *in vitro* model to explore the mechanism underlying the effects of tubulin palmitoylation on oocytes. We found that tubulin palmitoylation was decreased in HEK293T cells overexpressing PPT1 (Fig. 6E). Melatonin elevated tubulin palmitoylation in aged ovaries (Fig. 6B), 2BP-treated cells (Fig. 6D), D-gal-treated cells (Fig. S4C) and oePPT1-treated cells (Fig. 6E). These results demonstrate that melatonin can rescue the excessive depalmitoylation of tubulin mediated by PPT1 in aged mice.

To investigate the effect of PPT1 on tubulin function via the regulation of tubulin palmitoylation, we first explored the palmitoylation sites of tubulin targeted by PPT1. Cys12(β) and Cys354(β) play important roles in maintaining the structure and function of tubulin [36]. Therefore, we speculated that the decrease in tubulin palmitoylation induced by PPT1 might lead to abnormal tubulin distribution and polymerization. We analyzed the expression of tubulin on the membrane and in the cytoplasm of ovaries and HEK293T cells. Tubulin expression in the cytoplasm increased in the ovaries of aged mice and mice in the oePPT1 group but decreased after melatonin treatment, while the opposite changes in tubulin expression were observed in the membrane (Fig. 6F and G). The results of tubulin polymerization analysis showed that excessive polymerization of tubulin could be caused by the palmitoylation inhibitor 2BP and rescued by melatonin or palmitic acid (PA; Fig. 6H–I and Fig. S4D).

3. Discussion

In the present study, we investigated the role of PPT1 in oocyte aging via the regulation of tubulin depalmitoylation. In addition, melatonin was shown to improve the quality of aged oocytes by antioxidation and regulating PPT1 degradation.

In recent studies, ROS serves as a crucial factor in regulating Protein acyltransferase (PATs), such as ZDHHC5 and ZDHHC9, thereby modulating protein palmitoylation [11,37]. We found that ROS could also cause changes in palmitoylation in oocytes, but unlike in inflammation-related studies [11,38], excessive ROS in oocytes caused a decrease in globe protein palmitoylation by regulating PPT1. We hypothesize that this may be attributed to the differential impact of ROS on various PATs or depalmitoylases in different cells and culture conditions.

Melatonin exhibits multifaceted protective mechanisms on oocytes, encompassing antioxidant stress responses [39], maintenance of mitochondrial function [40], regulation of endoplasmic reticulum function [32], and protection of spindles [41]. However, its role in the regulation of protein palmitoylation has not been reported. In this study, we have uncovered that melatonin not only reduces ROS levels and improves lysosomal functions, but also directly binds to PPT1 and facilitates its degradation. These multiple effects collectively contribute to melatonin's rescuing effect on the hypo-palmitoylation state of aged oocytes. This discovery reveals a novel mechanism by which melatonin protects oocytes. Notably, melatonin reversed the adverse effects of 2BP on spindle assembly and microtubule polymerization. As 2BP is an inhibitor of ZDHHCs, but not an activator of PPT1, this result indicates that the regulatory effect of melatonin on palmitoylation may not be entirely dependent on PPT1. We believe that the mechanism by which melatonin regulates protein palmitoylation deserves more in-depth investigation.

The expression of PPT1 was significantly greater in the oocytes and ovaries of aged mice than in those of young mice, which has not been previously reported. In addition, we found that high oxidative stress may be one of the reasons for the up-regulation of PPT1 at advanced age. Interestingly, in our previous study, we also found that the expression of PPT1 is increased in the ovaries of PCOS patients [23], which exist ROS accumulation [42]. These finding implies that ROS-induced PPT1 overexpression may be closely related to female infertility. It was previously reported that PPT1 is localized in granulosa cells, cumulus cells and oocytes [43]. The increased PPT1 in aged mouse and postmenopausal human ovaries suggested that PPT1 might also contribute to

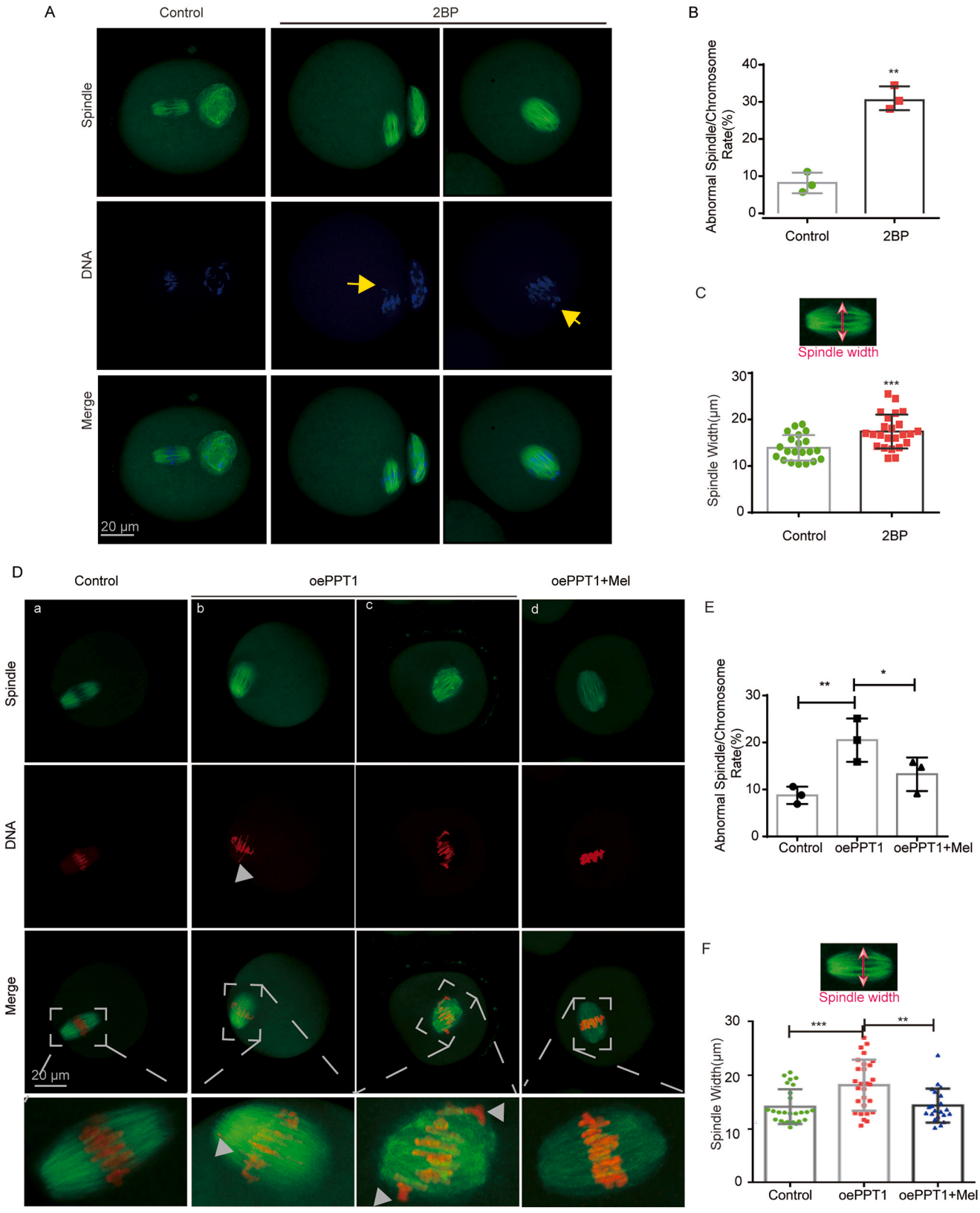

Fig. 4. 2BP and overexpressed PPT1 affects mouse oocyte spindle organization. (A) Oocytes in the control and 2BP groups were collected and stained to visualize spindles (green) and chromosomes (blue). Scale bar, 20 μm. (B) Quantitative analysis of control (n = 119) and 2BP (n = 101) oocytes with spindle defects or chromosome misalignment. (C) Quantitative analysis of spindle width in control (n = 21) and 2BP (n = 24) oocytes. (D) Oocytes from the control, oePPT1 and oePPT1 + mel groups were collected and stained to visualize spindles (green) and chromosomes (red). Aberrant spindles (arrows) and misaligned chromosomes (arrowheads) were readily observed in oePPT1 oocytes. Scale bar, 20 μm. (E) Quantitative analysis of oocytes from the control (n = 116), oePPT1 (n = 104) and oePPT1 + mel (n = 120) groups with spindle defects or chromosome misalignment. (F) Quantitative analysis of spindle width in control (n = 26), oePPT1 (n = 28) and oePPT1 + mel (n = 21) oocytes. The data are presented as the means ± SDs from three independent experiments. $^{*}p < 0.05$, $^{**}p < 0.01$, and $^{***}p < 0.001$.

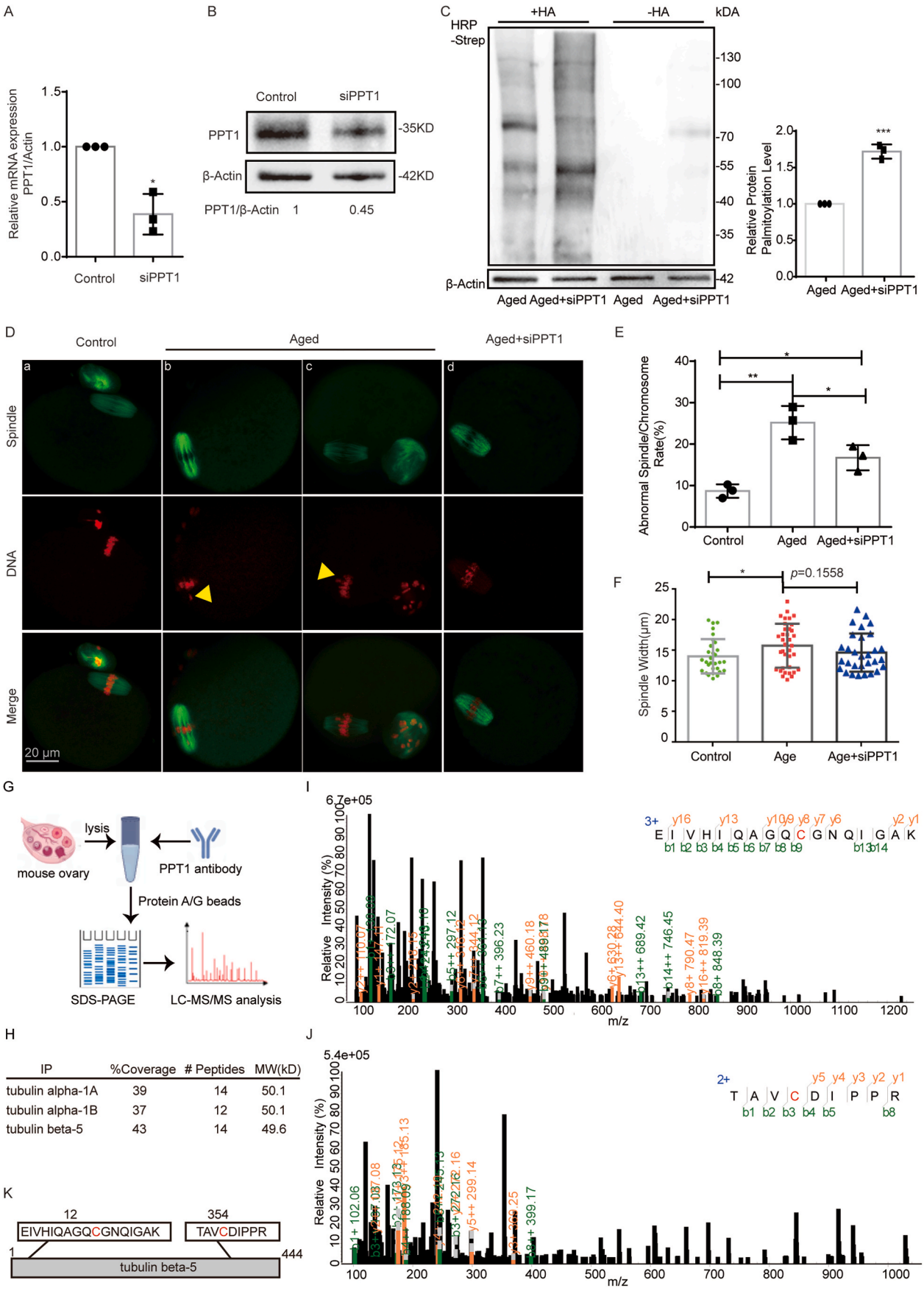

(caption on next page)

Fig. 5. Maternal age-associated oocyte spindle and chromosome abnormalities were suppressed by PPT1 knockdown and tubulin was detected to bind PPT1 by mass spectrometry. (A) The relative mRNA level of PPT1 in control and siPPT1 oocytes was determined by quantitative RT-PCR. (B) Western blot analysis showing PPT1 expression in control and siPPT1-treated oocytes. (C) Analysis of the palmitoylation levels of proteins extracted from aged and aged + siPPT1 oocytes. (D) Oocytes in the control, aged and aged + siPPT1 groups were collected and stained to visualize spindles (green) and chromosomes (red). Scale bar, 20 μm. (E) Quantitative analysis of oocytes in the control (n = 116), aged (n = 116) and aged + siPPT1 (n = 117) groups with spindle defects or chromosome misalignment. (F) Quantitative analysis of spindle width in control (n = 30), aged (n = 36) and aged + siPPT1 (n = 30) oocytes. (G) Schematic of mass spectrometry detection of PPT1-binding proteins. (H) Analysis of the binding of PPT1 to tubulin alpha 1A, tubulin alpha 1B and tubulin beta 5 by mass spectrometry. (I, J) Representative spectrum for the tubulin beta 5 peptide. (K) Schematic representation of tubulin palmitoylation sites identified by mass spectrometry. Actin served as a loading control for Western blotting and ABE assay. The data are presented as the means ± SDs from three independent experiments. $*p < 0.05$, $**p < 0.01$.

other dysfunctions in the ovary. PPT1 has been reported in fibroblasts [44] and immune cells (especially macrophages [45]), which are contained within the ovarian stroma. Therefore, we hypothesized that the increased number of fibroblasts and macrophages in the postmenopausal ovary may also contribute to the increased expression of PPT1. Melatonin has been reported to regulate macrophage function [46] and inhibit cancer-associated fibroblasts [47]. However, whether it can affect the expression of PPT1 in macrophages and fibroblasts in aging ovaries remains to be further studied.

The fact that PPT1 localizes at the spindle during oocyte meiosis and that PPT1 overexpression caused spindle defects are the main reasons that we focused on the changes in tubulin palmitoylation. Spindle assembly is a key step in oocyte maturation and aging, and a well-formed spindle is an indicator of oocyte quality [48]. Microtubules, which participate in the formation of spindles, have important biological functions, such as maintaining cell morphology and structure and participating in cell movement, intracellular material transport, signal transduction, and cell division. Tubulin is the main protein that constitutes microtubules. Posttranslational modification is a major contributor to microtubule diversity. The palmitoylation of tubulin ensures its membrane localization [49], and its attachment to the plasma membrane occurs via the palmitoyl moiety [50,51]. Consistently, the amount of tubulin on the membrane also corresponded to the tubulin palmitoylation level in our study.

In addition, tubulin palmitoylation finely controls microtubule dynamic instability and spindle assembly. Decreased tubulin palmitoylation can disrupt MT instability and cause spindle defects during mitosis [52]. Therefore, we hypothesized that decreased palmitoylation of tubulin may be an important cause of spindle defects during meiosis. Zhao et al. identified 11 palmitoylated cysteine residues of the α/β tubulin heterodimer, including 12(β) and 354(β), in the rat brain by nano-LC-MS/MS analysis [53]; these sites were identified as potential palmitoylation sites targeted by PPT1. Previous studies have shown that Cys12(β) is located in the GDP-binding region. The polymerization and depolymerization of tubulin are related to the conversion of GTP to GDP. Modification of Cys12 and Cys354 disrupts the interaction between β-tubulin and GTP, causes excessive polymerization of microtubules and affects spindle function [54,55]. In a cell-free tubulin assembly assay, we found that excessive 2BP promoted tubulin assembly. This result also suggested that overexpression of PPT1 results in abnormal enlargement and widening of the spindle. Moreover, PA was found to inhibit tubulin assembly into microtubule processes (Fig. 6I), suggesting that both excessive and insufficient tubulin palmitoylation can affect the normal polymerization of microtubules. In conclusion, our study revealed a new association between redox and palmitoylation in aging oocytes. Furthermore, we investigated the impact of PPT1 on oocyte aging, and our findings have illuminated a previously unknown mechanism underlying melatonin's function. These discoveries also indicate that palmitoylation represents a promising therapeutic target for addressing oocyte aging.

4. Materials and methods

4.1. Animals and diet

All animal experiments were reviewed by the Ethics Committee of Jinling Hospital (2022DZGKJDWLS-00149) and conducted according to the NIH Guide for the Care and Use of Laboratory Animals. Young control (6–8 weeks old) and aged (8–10 months old) female ICR mice were obtained from the Experimental Animal Center of Nanjing Medical University, housed at room temperature (22 ± 2 °C) and humidity (40–70 %) with lights on from 8:00 to 20:00 every day, and provided with pure-grade feed and water. The aged mice were randomly divided into two groups. One group (the aged + mel/i.g. group) received oral melatonin (Sigma, M5250) at 30 mg/kg body weight in corn oil daily at 6:00 p.m. for 21 days before ovary or oocyte collection [31]. The control and aged groups were treated with the same amount of corn oil.

4.2. Determination of serum hormone levels

Blood samples were collected by enucleation of the eyeball immediately after anesthesia, and serum was obtained by centrifugation for 10 min at 1000×*g*. Serum melatonin, estradiol (E2), progesterone (P), luteinizing hormone (LH), follicle-stimulating hormone (FSH) and AMH levels were assessed by commercial ELISA kits from Shanghai MLBIO Biotechnology Co., Ltd. (Shanghai, China) according to the manufacturer's instructions.

4.3. Oocyte collection and culture

Female ICR mice were superovulated by injecting 5 IU pregnant mare serum gonadotropin (PMSG). Approximately 46–48 h later, the mice were sacrificed and fully grown GV oocytes were collected by manually rupturing the antral ovarian follicles and placed in M2 medium (Sigma, M7161). After the cumulus cells were removed by repeated pipetting in 1 mg/ml hyaluronidase medium, the GV oocytes were cultured in M16 medium (Sigma, M7292) containing mineral oil at 37 °C in a 5 % CO_2 incubator. For *in vitro* treatment, 1 μM melatonin or 50 μM hydrogen peroxide (H_2O_2) was added to the M16 medium during IVM. 25, 50 and 100 μM 2BP were added to M16 medium for dose selection. Contrast images of MII oocytes from the control and 2BP groups were acquired with a camera on a stereomicroscope (IX73, Olympus Corporation, Japan) with a 20 × objective.

4.4. HE staining and follicle counting

For the assessment of follicle number, standard Hematoxylin and Eosin (HE) staining was employed. Briefly, ovaries were fixed in 4 % formalin, embedded in paraffin, and sectioned at a thickness of 5 μm. Every fifth section was collected for HE staining. The sections were then subjected to dewaxing, hydration, staining with Hematoxylin for 5 min followed by Eosin for 2 min, dehydration, clearing, and mounting. Finally, the slides were observed and follicle counts were performed using IX-73 microscope (Olympus Corporation, Tokyo, Japan) at the appropriate magnification.

4.5. Human ovary and follicular fluid collection

This human study was approved by the Ethics Committee of Jinling Hospital (2022DZGDR-035) and was performed in accordance with national and international guidelines. Three young (aged 27–30 years) and three aged (aged 54–57 years) Chinese women who underwent

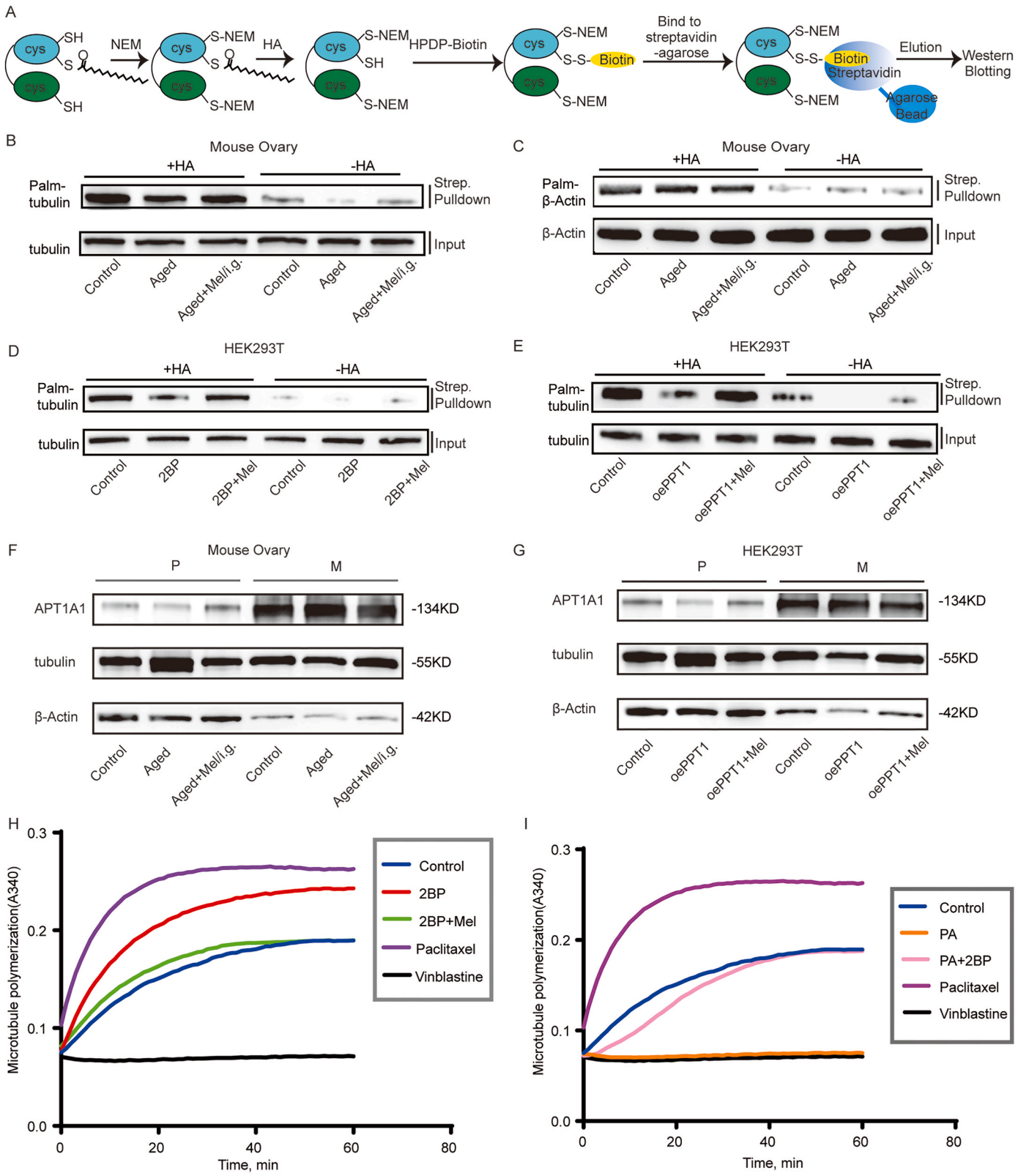

Fig. 6. Effects of tubulin depalmitoylation on tubulin function. (A) Schematic of ABE for detecting protein palmitoylation. (B, C) Measurement of palmitoylation levels of tubulin and actin in the control, aged and aged + mel/i.g. mouse ovaries. (D) Measurement of tubulin palmitoylation levels in HEK293T cells in the control, 2BP and 2BP + mel groups. (E) Measurement of tubulin palmitoylation levels in HEK293T cells in the control, oePPT1 and oePPT1 + mel groups. (F) Analysis of tubulin expression in the membrane and cytoplasm of control, aged and aged + mel/i.g. mouse ovaries. M, membrane; P, cytoplasm. (G) Analysis of tubulin expression in the membrane and cytoplasm of HEK293T cells in the control, oePPT1 and oePPT1 + mel groups. M, membrane; P, cytoplasm. (H, I) The polymerization of tubulin in the different groups was assessed by a cell-free tubulin assembly assay.

bilateral salpingo-oophorectomy because of benign ovarian tumors or uterine diseases were recruited. Partial removal of the ovaries was performed, and the ovaries were cryopreserved for subsequent experiments.

The follicular fluid samples were collected from women undergoing oocyte retrieval for IVF/ICSI at the Department of Reproductive Medicine, Jinling Hospital between March 2024 and August 2024. Participants were required to meet the following requirements: 1) age between 20 and 50 years old; 2) unable to conceive naturally for at least 1 year, regardless of male, female, both, or uncertain factors; 3) primary or secondary infertility; and 4) IVF or ICSI cycles fertilized by husband or donor sperm. Participants with polycystic ovary syndrome, premature ovarian failure, endometriosis, and other reproductive endocrine diseases, such as thyroid disease, diabetes, adrenal disease, etc., were excluded. A total of 56 Chinese females were recruited. Among the donors, those age ≤35 years and AMH >1.2 ng/mL were named as the control group, those age >35 years and AMH >1.2 ng/mL and antral follicle count (AFC) > 5 were named as the aged-control group, and those age >35 years, AMH <1.2 ng/mL and AFC ≤5 were named as the aged-DOR group.

4.6. PPT1 overexpression and knockdown

Microinjections of mRNA or siRNA with a Narishige (Tokyo, Japan) microinjector were used to overexpress or knock down PPT1 in mouse oocytes, respectively.

For the overexpression experiments, PPT1 mRNA was synthesized. The HA-PPT1 plasmid was purchased from Gene Create Biological Engineering Co., Ltd. (Wuhan, China). The plasmid carrier was pcDNA3.1 (+), and the gene sequence number was NM_008917.3. The HA-PPT1 plasmid was digested by the restriction endonuclease XhoI (TAKARA, 1094S) to form linearized double-stranded DNA, which was used as a template for mRNA transcription *in vitro*. After *in vitro* transcription using the mMESSAGE mMACHINE®T7 Ultra Kit (Invitrogen, AM1345), mRNA separation and purification were performed using the MEGAclear Kit (Invitrogen, AM1909). Then, 10 pL PPT1 mRNA solution (700 ng/μL) was injected into the cytoplasm of GV oocytes. The same amount of RNase-free PBS was injected as a control.

For knockdown experiments, PPT1 siRNA was diluted with water to obtain a 25 μM stock solution, and then 2.5 pL of the solution was injected into the cytoplasm of fully grown immature oocytes. A random siRNA was injected as a control. The PPT1 siRNA sequences are shown in Supplementary Table 2.

After injection, the oocytes were transferred to M16 culture medium containing 2.5 μM milrinone (Sigma, M4659) for 20 h to induce the overexpression or knockdown of PPT1 mRNA.

4.7. HEK293T cell culture and transfection

Human HEK293T cells were cultured in basic DMEM (Gibco, 11965-092) supplemented with 10 % fetal bovine serum (FBS; HAKATA, HN-FBS-50), 1 % (vol/vol) penicillin/streptomycin (Gibco, 15140-122) and 2 % trimethoprim (InvivoGen, Ant-nr-1). The incubator temperature was 37 °C, the concentration of carbon dioxide was 5 %, and the humidity was 5 %. HEK293T cells were transiently transfected with Liposome 3000 reagent (Invitrogen, L3000075) according to the manufacturer's instructions. Follow-up experiments were performed 24–48 h after transfection.

4.8. Immunofluorescence

Oocytes were fixed in 4 % PFA for 30 min at room temperature and permeabilized with 0.5 % Triton X-100 for 20 min. The oocytes were then blocked in 1 % BSA for 1 h at room temperature and incubated overnight with the following primary antibodies at 4 °C: an anti-PPT1 antibody (Invitrogen, PA5-29177; 1:100) or anti-Lamp1 antibody (Abclonal, A23947; 1:100) or a FITC-conjugated anti-tubulin antibody (Sigma, F2168; 1:250) or Rabbit Serum (Proteintech, B900760). After multiple washes with PBS, the oocytes were labeled with Rhodamine goat-anti-rabbit IgG (ZSGB-Bio, ZF-0316, 1:100) or FITC goat-anti-rabbit IgG (ZSGB-Bio, ZF-0311, 1:100) at room temperature for 1 h. Hoechst 33342 (Sigma, 14533; blue) or propidium iodide (PI; Sigma, P4170; red) was used for chromosome staining. Oocyte samples were mounted with anti-fade medium and then examined under a laser scanning confocal microscope (LSM810, Zeiss, Germany; FV3000, Olympus, Japan) equipped with a 40 × objective.

4.9. Western blotting

For oocyte protein extraction, approximately 100 oocytes were lysed in Laemmli sample buffer containing protease inhibitor and boiled for 5 min.

For tissue and cell protein extraction, ovarian tissues or HEK293T cells were placed in RIPA lysis buffer supplemented with 1 mM protease inhibitor, lysed with a tissue grinder, and boiled at 95 °C for 10 min, after which the supernatant was centrifuged (12000×*g*, 15 min, 4 °C). The protein concentration was determined by the BCA method.

The samples were separated on a 10 % SDS-PAGE gel and then transferred to PVDF membranes. The membranes were blocked with 5 % BSA at room temperature for 1 h and incubated with the following primary antibodies diluted to the appropriate concentration in a shaker at 4 °C overnight: anti-PPT1 antibody (1:3000), anti-actin antibody (Proteintech, 66009-1-Ig; 1:5000) and anti-tubulin antibody (Cell Signaling Technology, 2148s, 1:5000). The membranes were washed with TBST the next day and incubated at room temperature with HRP-conjugated secondary antibodies. The protein bands were visualized using an ECL Plus Western blotting Detection System (Abbkine, BMU102-CB). ImageJ software (NIH) was used to analyze the gray values of the bands and to calculate the expression ratio of each protein.

4.10. Molecular docking analysis

The molecular structures of melatonin was retrieved from PubChem Compound (http://pubchem.ncbi.nlm.nih.gov/) and 3D coordinates of PPT1 (PDB ID, 3GRO) was downloaded from the PDB (http://www.rcsb.org/pdb/home/home.do). The project preformed by Antodock Vina v.1.2.2 (http://autodock.scipps.edu/).

4.11. Surface Plasmon Resonance (SPR) assay

The activator was prepared by mixing 400 mM EDC and 100 mM NHS (GE) immediately prior to injection. The mixture was injected 800 s to Fc1 and Fc2 sample channel at a flow rate of 10 μL/min 20 μg/mL of PPT1(MCE, HY-P700622) in 10 mM NaAc (pH 4.0) was then injected 1700 s to Fc2 sample channel at a flow rate of 10 μL/min, the immobilization level of about 4884RU. The chip was deactivated by 1 M Ethanolamine hydrochloride (GE) at a flow rate of 10 μL/min for 800 s into Fc1 and Fc2 sample channel.

Dilute Melatonin with the Running Buffer (1 × PBS-P 5 %DMSO Buffer, GE) to 8 concentrations (2500, 1250, 625, 312.50, 156.25, 78.13, 39.06, 19.53 and 0 μM). The Melatonin is injected to Fc1-Fc2 of channel at a flow rate of 30 μL/min for an association phase of 60 s, followed by 90 s dissociation. The association and dissociation process are all handling in the Running Buffer.

4.12. Acyl-biotin exchange (ABE) assay

Protein palmitoylation was assessed by an ABE Assay. For analysis of total protein palmitoylation, the BMCC-biotin method was used as described in articles on palmitoylation previously published by our laboratory [23,35].

The HPDP-biotin method was also used to analyze the palmitoylation

levels of specific proteins. Treated HEK293T cells or ovarian tissue were collected and analyzed as described in published articles [23,35]. Then, the samples were analyzed by western blotting.

4.13. Quantitative real-time PCR

Total RNA was isolated from oocytes using an RNA Isolation Kit (Invitrogen, KIT0204), and cDNA levels were quantified by quantitative RT-PCR (Abbkine, BMU102-CB) using the Roche Light Cycler 96 Real-Time PCR System (Roche Diagnostics, Basel, Switzerland). Thirty oocytes were used in each group for a single experiment. β-Actin was used as the internal reference to calculate the fold change in *PPT1* expression with the $2^{-\Delta\Delta Ct}$ method. The mRNA level in control oocytes was set to 1. The sequences of the primers utilized were provided in Supplementary Table 3.

4.14. Mass spectrometry analysis

Mouse ovaries were crushed with a tissue grinder in RIPA lysis buffer supplemented with 1 mM protease inhibitor and then centrifuged (12000×*g*, 15 min, 4 °C) to obtain cell lysates. The cell lysates were immunoprecipitated with an anti-PPT1 antibody bound to protein A/G magnetic beads (Selleck, B23202) (4 °C, overnight). The beads were washed three times with lysis buffer, and the proteins were separated by SDS-PAGE and then stained with Coomassie blue (KeyGEN, KGP1004). The entire lane was excised and digested with trypsin in 25 mM NH_4HCO_3 at 37 °C for 20 h. The peptides were extracted three times with 60 % acetonitrile (ACN)/0.1 % trifluoroacetic acid (TFA), pooled and dried completely by a vacuum centrifuge. Chromatography-tandem mass spectrometry (LC-MS/MS) analysis was performed by Applied Protein Technology (Aptbiotech, Inc. Shanghai, China).

4.15. Separation of cell membrane and plasma proteins

A Nuclear and Cytoplasmic Protein Extraction Kit (Beyotime, P0028) was used. The membrane protein extraction reagents A and B were dissolved, mixed at room temperature and then placed on melted ice. PMSF was added to extraction reagents A and B right before the experiment at a final concentration of 1 mM. Ovarian tissue or cells were washed with PBS, and 1 mL of membrane protein extraction reagent A was added. The samples were incubated on ice for 15 min and freeze-thawed in liquid nitrogen for lysis, and the supernatant was collected in a new 1.5 mL centrifuge tube after centrifugation at low speed. The supernatant was then centrifuged at 4 °C and 14000×*g* for 30 min, and the resulting supernatant was collected as the cytoplasmic protein fraction, which was stored at −80 °C until use. As much of the supernatant as possible was removed from the pellet and discarded Then, 200 μL of membrane protein extraction reagent B was added to the pellet, and the mixture was swirled for 5 s, placed on ice for 10 min, vortexed and placed in an ice bath twice. After centrifugation at 4 °C and 14000×*g* for 15 min, the supernatant was collected as the cell membrane protein fraction.

4.16. Tubulin polymerization assay

The tubulin polymerization assay was performed with a tubulin polymerization assay kit (Cytoskeleton, BK006P) according to the manufacturer's instructions. Briefly, the tubulin was diluted with 420 μL of ice cold tubulin polymerization buffer containing 80 mM PIPES pH 6.9, 2 mM $MgCl_2$, 0.5 mM EGTA, 1 mM GTP, 10.2 % glycerol to give a final concentration of 3 mg/mL tubulin. Then, the diluted tubulin was transferred to the pre-warm 96-well plate and mixed with paclitaxel (30 μmol/L), vincristine (3 μmol/L), 2BP (3 μmol/L), melatonin (3 μmol/L), PA (3 μmol/L) or DMSO at a final concentration of 0.1 %; DMSO served as the solvent control. The polymerization of tubulin was measured at each consecutive minute during a period of 30 min at 37 °C using the microplate reader (SynergyHTX, BioTek Instruments Inc., USA) set at 360 nm.

4.17. Statistical analysis

All data in this study were statistically analyzed and graphed using GraphPad Prism 6.0 software. The measurement data were normally distributed and are expressed as the mean ± SD. For the percentage data, arcsine transformation was applied before statistical analysis. A *t*-test was used to compare the two groups. One-way ANOVA was used to compare the data from each group with the control. Different groups were compared using one-way analyses of variance followed by the least significant difference (equal variances) or Games-Howell (unequal variances) post hoc test. $p < 0.05$ was considered to indicate statistical significance (ns means $p > 0.05$, * means $p < 0.05$, ** means $p < 0.01$, *** means $p < 0.001$, **** means $p < 0.0001$).

CRediT authorship contribution statement

Rujun Ma: Writing – original draft, Project administration, Funding acquisition, Data curation. **Mengqi Xue:** Writing – original draft, Methodology, Investigation, Data curation. **Feiyan Ge:** Investigation. **Kadiliya Jueraitetibaike:** Resources, Investigation, Funding acquisition. **Shanmeizi Zhao:** Project administration, Data curation. **Zhang Qian:** Investigation, Data curation. **Zhaowanyue He:** Supervision, Resources. **Hong Zhang:** Supervision, Project administration. **Ting Tang:** Resources. **Chun Cao:** Investigation. **Chuwei Li:** Supervision, Project administration. **Lu Zheng:** Resources, Data curation. **Tongmin Xue:** Data curation. **Jie Dong:** Funding acquisition. **Jun Jing:** Supervision, Project administration. **Jian Zhong:** Resources, Conceptualization. **Jinzhao Ma:** Supervision, Project administration. **Yang Yang:** Resources. **Yadong Huang:** Writing – review & editing, Project administration, Funding acquisition. **Xie Ge:** Writing – review & editing, Validation, Supervision, Project administration, Conceptualization. **Bing Yao:** Writing – review & editing, Supervision, Funding acquisition, Conceptualization. **Li Chen:** Writing – review & editing, Supervision, Project administration, Investigation, Funding acquisition, Data curation, Conceptualization.

Declaration of competing interest

The authors declare that they have no known competing financial interests or personal relationships that could have appeared to influence the work reported in this paper.

Acknowledgments

This work was supported by the National Natural Science Foundation of China (82271687, 82301869, U22A20277, 82274651, 81973965, 32000583 and 81971373), the Jiangsu Key Research and Development Program (BE2022712), the Key Project of Medical Scientific Research of Jiangsu Commission of Health (ZD2022004), and Jiangsu Provincial Medical Key Discipline Cultivation Unit (JSDW202215).

Appendix A. Supplementary data

Supplementary data to this article can be found online at https://doi.org/10.1016/j.redox.2025.103510.

Data availability

Data will be made available on request.

References

[1] K. Kikuchi, K. Naito, J. Noguchi, H. Kaneko, H. Tojo, Maturation/M-phase promoting factor regulates aging of porcine oocytes matured in vitro, Clon Stem Cell 4 (2002) 211–222, https://doi.org/10.1089/15362300260339494.

[2] Y.L. Miao, K. Kikuchi, Q.Y. Sun, H. Schatten, Oocyte aging: cellular and molecular changes, developmental potential and reversal possibility, Hum. Reprod. Update 15 (2009) 573–585, https://doi.org/10.1093/humupd/dmp014.

[3] X.F. Ye, et al., Caffeine and dithiothreitol delay ovine oocyte ageing, Reprod. Fertil. Dev. 22 (2010) 1254–1261, https://doi.org/10.1071/RD10062.

[4] R. Ma, Y. Zhang, L. Zhang, J. Han, R. Rui, Sirt1 protects pig oocyte against in vitro aging, Animal science journal = Nihon chikusan Gakkaiho 86 (2015) 826–832, https://doi.org/10.1111/asj.12360.

[5] T.A. Ahmed, et al., Oocyte aging: the role of cellular and environmental factors and impact on female fertility, Adv. Exp. Med. Biol. 1247 (2020) 109–123, https://doi.org/10.1007/5584_2019_456.

[6] X. Ge, et al., Protein palmitoylation-mediated palmitic acid sensing causes blood-testis barrier damage via inducing ER stress, Redox Biol. 54 (2022) 102380, https://doi.org/10.1016/j.redox.2022.102380.

[7] L. Sui, S. Zhang, R. Huang, Z. Li, HDAC11 promotes meiotic apparatus assembly during mouse oocyte maturation via decreasing H4K16 and alpha-tubulin acetylation, Cell Cycle 19 (2020) 354–362, https://doi.org/10.1080/15384101.2019.1711315.

[8] G. Sendzikaite, G. Kelsey, The role and mechanisms of DNA methylation in the oocyte, Essays Biochem. 63 (2019) 691–705, https://doi.org/10.1042/EBC20190043.

[9] P. Yuan, et al., UCH-L1 inhibitor LDN-57444 hampers mouse oocyte maturation by regulating oxidative stress and mitochondrial function and reducing ERK1/2 expression, Biosci. Rep. 40 (2020), https://doi.org/10.1042/BSR20201308.

[10] E. Ziemlinska, et al., Palm oil-rich diet affects murine liver proteome and S-palmitoylome, Int. J. Mol. Sci. 22 (2021), https://doi.org/10.3390/ijms222313094.

[11] Gang Du, B.H. L, Liron David, Caitlin Walker, Tarick J. El-Baba, Corinne A. Lutomski, Byoungsook Goh, Bowen Gu, Xiong Pi, Pascal Devant, Pietro Fontana, Ying Dong, Xiyu Ma, Rui Miao, Arumugam Balasubramanian, Puthenveetil Robbins, Anirban Banerjee, Hongbo R. Luo, Jonathan C. Kagan, Sungwhan F. Oh, Carol V. Robinson, Judy Lieberman, Hao Wu, ROS-dependent S-palmitoylation activates cleaved and intact gasdermin D, Nature (2024), https://doi.org/10.1038/s41586-024-07373-5.

[12] R. Guo, et al., Reduction of DHHC5-mediated beclin 1 S-palmitoylation underlies autophagy decline in aging, Nat. Struct. Mol. Biol. 31 (2024) 232–245, https://doi.org/10.1038/s41594-023-01163-9.

[13] Y.Z. Mengyuan Qu, Qing Xingrong, Xinzong Zhang, Honggang Li, Androgen-dependent miR-125a-5p targets LYPLA1 and regulates global protein palmitoylation level in late-onset hypogonadism males, J. Cell. Physiol. 236 (2021) 4738–4749, https://doi.org/10.1002/jcp.30195.

[14] T. Dudler, M.H. Gelb, Palmitoylation of Ha-Ras facilitates membrane binding, activation of downstream effectors, and meiotic maturation in Xenopus oocytes, J. Biol. Chem. 271 (1996) 11541–11547, https://doi.org/10.1074/jbc.271.19.11541.

[15] J. Fang, et al., Involvement of protein acyltransferase ZDHHC3 in maintaining oocyte meiotic arrest in Xenopus laevis, Biol. Reprod. 95 (2016) 67, https://doi.org/10.1095/biolreprod.116.138941.

[16] M.X. Henderson, et al., Neuronal ceroid lipofuscinosis with DNAJC5/CSPalpha mutation has PPT1 pathology and exhibit aberrant protein palmitoylation, Acta Neuropathol. 131 (2016) 621–637, https://doi.org/10.1007/s00401-015-1512-2.

[17] L.A. Camp, S.L. Hofmann, Purification and properties of a palmitoyl-protein thioesterase that cleaves palmitate from H-Ras, J. Biol. Chem. 268 (1993) 22566–22574.

[18] J. Jin, X. Zhi, X. Wang, D. Meng, Protein palmitoylation and its pathophysiological relevance, J. Cell. Physiol. 236 (2021) 3220–3233, https://doi.org/10.1002/jcp.30122.

[19] J. Vesa, et al., Mutations in the palmitoyl protein thioesterase gene causing infantile neuronal ceroid lipofuscinosis, Nature 376 (1995) 584–587, https://doi.org/10.1038/376584a0.

[20] Z. Zhang, et al., Palmitoyl-protein thioesterase-1 deficiency mediates the activation of the unfolded protein response and neuronal apoptosis in INCL, Hum. Mol. Genet. 15 (2006) 337–346, https://doi.org/10.1093/hmg/ddi451.

[21] C.A. Korey, M.E. MacDonald, An over-expression system for characterizing Ppt1 function in Drosophila, BMC Neurosci. 4 (2003) 30, https://doi.org/10.1186/1471-2202-4-30.

[22] Y. Liu, et al., Palmitoyl-protein thioesterase 1 (PPT1): an obesity-induced rat testicular marker of reduced fertility, Mol. Reprod. Dev. 81 (2014) 55–65, https://doi.org/10.1002/mrd.22281.

[23] T. Xue, et al., PPT1 regulation of HSP90alpha depalmitoylation participates in the pathogenesis of hyperandrogenism, iScience 26 (2023) 106131, https://doi.org/10.1016/j.isci.2023.106131.

[24] H.R. Yun, et al., Palmitoyl protein thioesterase 1 is essential for myogenic autophagy of C2C12 skeletal myoblast, Front. Physiol. 11 (2020) 569221, https://doi.org/10.3389/fphys.2020.569221.

[25] L. Wang, et al., Oxidative stress in oocyte aging and female reproduction, J. Cell. Physiol. 236 (2021) 7966–7983, https://doi.org/10.1002/jcp.30468.

[26] J. van der Reest, G. Nardini Cecchino, M.C. Haigis, P. Kordowitzki, Mitochondria: their relevance during oocyte ageing, Ageing Res. Rev. 70 (2021) 101378, https://doi.org/10.1016/j.arr.2021.101378.

[27] R.J. Reiter, D.X. Tan, A. Galano, Melatonin: exceeding expectations, Physiology 29 (2014) 325–333, https://doi.org/10.1152/physiol.00011.2014.

[28] R.J. Reiter, et al., Aging-related ovarian failure and infertility: melatonin to the rescue, Antioxidants 12 (2023), https://doi.org/10.3390/antiox12030695.

[29] H. Tamura, et al., Importance of melatonin in assisted reproductive Technology and ovarian aging, Int. J. Mol. Sci. 21 (2020), https://doi.org/10.3390/ijms21031135.

[30] M. Zhang, Y. Lu, Y. Chen, Y. Zhang, B. Xiong, Insufficiency of melatonin in follicular fluid is a reversible cause for advanced maternal age-related aneuploidy in oocytes, Redox Biol. 28 (2020) 101327, https://doi.org/10.1016/j.redox.2019.101327.

[31] C. Li, et al., Melatonin ameliorates the advanced maternal age-associated meiotic defects in oocytes through the SIRT2-dependent H4K16 deacetylation pathway, Aging 12 (2020) 1610–1623, https://doi.org/10.18632/aging.102703.

[32] H. Zhang, et al., Melatonin improves the quality of maternally aged oocytes by maintaining intercellular communication and antioxidant metabolite supply, Redox Biol. 49 (2022) 102215, https://doi.org/10.1016/j.redox.2021.102215.

[33] Q. Yang, et al., NADase CD38 is a key determinant of ovarian aging, Nature aging 4 (2024) 110–128, https://doi.org/10.1038/s43587-023-00532-9.

[34] K. Jueraitetibaike, et al., MiR-425-5p suppression of Crebzf regulates oocyte aging via chromatin modification, GeroScience 46 (2024) 3723–3742, https://doi.org/10.1007/s11357-023-00875-6.

[35] K. Liang, et al., miR-125a-5p increases cellular DNA damage of aging males and perturbs stage-specific embryo development via Rbm38-p53 signaling, Aging Cell 20 (2021) e13508, https://doi.org/10.1111/acel.13508.

[36] H.T. Seki T, T. Hosono-Fukao, K. Inada, R. Tanaka, J. Ogihara, T. Ariga, Anticancer effects of diallyl trisulfide derived from garlic, Asia Pac. J. Clin. Nutr. 17 (Suppl 1) (2008) 249–252.

[37] L. Chen, et al., Palmitoylation alters LDHA activity and pancreatic cancer response to chemotherapy, Cancer Lett. 587 (2024) 216696, https://doi.org/10.1016/j.canlet.2024.216696.

[38] H.A. Balasubramanian A, L. Ghimire, M. Tahir, P. Devant, P. Fontana, G. Du, X. Liu, D. Fabin, H. Kambara, X. Xie, F. Liu, T. Hasegawa, R. Xu, H. Yu, M. Chen, S. Kolakowski, S. Trauger, M.R. Larsen, W. Wei, H. Wu, J.C. Kagan, J. Lieberman, H.R. Luo, The palmitoylation of gasdermin D directs its membrane translocation and pore formation during pyroptosis, Sci. Immunol. 9 (2024) eadn1452.

[39] C. Zhan, et al., Melatonin protects porcine oocyte from copper exposure potentially by reducing oxidative stress potentially through the Nrf2 pathway, Theriogenology 193 (2022) 1–10, https://doi.org/10.1016/j.theriogenology.2022.09.004.

[40] C. He, et al., Melatonin facilitates oocyte growth in goats and mice through increased nutrient reserves and enhanced mitochondrial function, Faseb. J. 38 (2024), https://doi.org/10.1096/fj.202400574R.

[41] M. Lan, et al., Melatonin protects against defects induced by deoxynivalenol during mouse oocyte maturation, J. Pineal Res. 65 (2018), https://doi.org/10.1111/jpi.12477.

[42] R. Ma, et al., Effects of n-3 PUFA supplementation on oocyte in vitro maturation in mice with polycystic ovary syndrome, J. Ovarian Res. 16 (2023) 87, https://doi.org/10.1186/s13048-023-01162-w.

[43] S. Uzbekova, et al., Protein palmitoylation in bovine ovarian follicle, Int. J. Mol. Sci. 22 (2021), https://doi.org/10.3390/ijms222111757.

[44] A. Lyly, et al., Glycosylation, transport, and complex formation of palmitoyl protein thioesterase 1 (PPT1)–distinct characteristics in neurons, BMC Cell Biol. 8 (2007) 22, https://doi.org/10.1186/1471-2121-8-22.

[45] J. Weng, et al., Intratumoral PPT1-positive macrophages determine immunosuppressive contexture and immunotherapy response in hepatocellular carcinoma, J. Immunotherapy Cancer 11 (2023), https://doi.org/10.1136/jitc-2022-006655.

[46] L. Du, et al., Melatonin shapes bacterial clearance function of porcine macrophages during enterotoxigenic Escherichia coli infection, Anim. Nutr. 11 (2022) 242–251, https://doi.org/10.1016/j.aninu.2022.06.018.

[47] H. Liao, et al., Melatonin blunts the tumor-promoting effect of cancer-associated fibroblasts by reducing IL-8 expression and reversing epithelial-mesenchymal transition, Int. Immunopharm. 119 (2023) 110194, https://doi.org/10.1016/j.intimp.2023.110194.

[48] J.R. Gruhn, et al., Chromosome errors in human eggs shape natural fertility over reproductive life span, Science 365 (2019) 1466–1469.

[49] A.M. Zambito, J. Wolff, Palmitoylation of tubulin, Biochem. Biophys. Res. Commun. 239 (1997) 650–654.

[50] J. Wolff, Plasma membrane tubulin, Biochim. Biophys. Acta 7 (2009) 26.

[51] A.M. Zambito, J. Wolff, Plasma membrane localization of palmitoylated tubulin, Biochem. Biophys. Res. Commun. 283 (2001) 42–47.

[52] C.T. Fang, et al., Inhibition of acetyl-CoA carboxylase impaired tubulin palmitoylation and induced spindle abnormalities, Cell Death Dis. 9 (2023) 23–1301.

[53] Z. Zhao, et al., Acyl-biotinyl exchange chemistry and mass spectrometry-based analysis of palmitoylation sites of in vitro palmitoylated rat brain tubulin, Protein J. 29 (2010) 531–537.

[54] W. Xu, et al., Natural product derivative Bis(4-fluorobenzyl)trisulfide inhibits tumor growth by modification of beta-tubulin at Cys 12 and suppression of microtubule dynamics, Mol. Cancer Therapeut. 8 (2009) 3318–3330.

[55] M.L. Gupta Jr., C.J. Bode, C.A. Dougherty, R.T. Marquez, R.H. Himes, Mutagenesis of beta-tubulin cysteine residues in Saccharomyces cerevisiae: mutation of cysteine 354 results in cold-stable microtubules, Cell Motil Cytoskeleton 49 (2001) 67–77.